



2D GEOMETRY OF QUADRAPOLE MAGNETIC FIELD LINES FROM NEUTRON STAR AND ASSOCIATED RADIATION PRESSURE

By
Melkameshet Girma

SUBMITTED IN PARTIAL FULFILLMENT OF THE
REQUIREMENTS FOR THE DEGREE OF
MASTER OF SCIENCE IN PHYSICS

AT
ADDIS ABABA UNIVERSITY
ADDIS ABABA, ETHIOPIA

JUNE 2011

ADDIS ABABA UNIVERSITY
DEPARTMENT OF
PHYSICS

Supervisor:

Dr. Legsse Wottro

Examiners:

Dr. Abraham Amaha

Dr. Gizaw Mengstu

ADDIS ABABA UNIVERSITY

Date: **JUNE 2011**

Author: **Melkameshet Girma**

Title: **2D Geometry Of Quadrapole Magnetic Field Lines
From Neutron Star And Associated Radiation pressure**

Department: **Physics**

Degree: **M.Sc.** Convocation: **JUNE** Year: **2011**

Permission is herewith granted to Addis Ababa University to circulate and to have copied for non-commercial purposes, at its discretion, the above title upon the request of individuals or institutions.

Signature of Author

THE AUTHOR RESERVES OTHER PUBLICATION RIGHTS, AND NEITHER THE THESIS NOR EXTENSIVE EXTRACTS FROM IT MAY BE PRINTED OR OTHERWISE REPRODUCED WITHOUT THE AUTHOR'S WRITTEN PERMISSION.

THE AUTHOR ATTESTS THAT PERMISSION HAS BEEN OBTAINED FOR THE USE OF ANY COPYRIGHTED MATERIAL APPEARING IN THIS THESIS (OTHER THAN BRIEF EXCERPTS REQUIRING ONLY PROPER ACKNOWLEDGEMENT IN SCHOLARLY WRITING) AND THAT ALL SUCH USE IS CLEARLY ACKNOWLEDGED.

Table of Contents

Table of Contents	v
List of Figures	vi
Abstract	vii
Acknowledgements	viii
1 INTRODUCTION	1
1.1 Neutron Star	1
1.1.1 Formation of Neutron Stars	1
1.1.2 Structure of Neutron Stars	2
1.1.3 Discoveries	3
1.1.4 Rotation	5
1.1.5 Magnetic Field	5
1.1.6 Magnetic Field	6
1.1.7 Conservetion of Magnetic Field	8
2 MAGNETIC FIELD LINE GEOMETRY	10
2.1 Expansion of Multipole Vector Potential	10
2.2 Dipole Vector Potential	12
2.3 Derivation of Magnetic Field	14
2.4 Magnetic Field Outside The Crust	16
2.5 Magnetic Field Line	18
2.6 Dipole Magnetic Field Line	18
2.7 Quadrupole Vector Potential	19
2.8 Quadrupole Magnetic Field	21
2.9 Quadrupole Magnetic Field line	22
3 MAGNETIC RADIATION	24
3.1 The Retarded Potential For An Oscillating Magnetic Dipole	24
3.2 Magnetic Dipole Radiation	26
3.3 Poynting Vector	27

3.4	Radiation Pressure Of Dipole Fields	28
3.5	Magnetic Quadrapole Radiation	29
4	CONCLUSION	34

List of Figures

1.1	The stacture of neutron star	3
1.2	Pulsars rotation axis, magnetic axis, and magnetic field	6
1.3	Magnetic flux conservation	8
2.1	Shows a field vector \mathbf{B} decomposed into the radial \mathbf{B}_r and polar \mathbf{B}_θ components	15
2.2	The geometry of field lines from magnetic dipole moment when $K_d = 1$	19
2.3	The geometry of the quadrupole field line where $K_Q = 1$	23
3.1	An oscillating magnetic dipole.	25
3.2	Polar diagram of $\sin^2 \theta$	28
3.3	The two dipoles magnetic moment	30
3.4	Polar diagram of $\sin^2 \theta \cos^2 \theta$	32

Abstract

In this thesis we have derived the vector potential to determine the analytic expressions for the magnetic field of dipole and quadrupole components of neutron star, we develop the field line equations and the magnetic field line geometry of both dipole and quadrupole terms. The magnetic field varies with time and as well as the induced electric field. As a result the neutron star can generate electromagnetic radiation. This electromagnetic radiation has pressure. We have derived the radiation pressure at any distance r out side of the surface of the neutron star.

Acknowledgements

I would like to express my sincere thanks to my advisor and instructor Dr. Legesse Wotro for his guidance, assistance, supervision and contribution of valuable suggestions. His scientific excitement, integral view on research and overly enthusiasm, has made a deep impression on me. I would like to thank all my friends and the astro-group members for providing encouragement and support.

Chapter 1

INTRODUCTION

1.1 Neutron Star

A neutron star is a type of stellar remnant that can result from the gravitational collapse of a massive star during a supernova event. Such stars are composed almost entirely of neutrons, which are subatomic particles without electrical charge and a slightly larger mass than protons. Neutron stars are very hot and are supported against further collapse because of the neutron degenerate pressure. A typical neutron star has a mass between 1.35 and about 2.0 solar masses, with a corresponding radius of about 12 km. In contrast, the Sun's radius is about 60,000 times that. Neutron stars have overall densities of 3.7×10^{17} to $5.9 \times 10^{17} \text{ kg/m}^3$ (2.6×10^{14} to 4.1×10^{14} times the density of the Sun), which compares with the approximate density of an atomic nucleus of $3 \times 10^{17} \text{ kg/m}^3$. The neutron star's density varies from below $1 \times 10^9 \text{ kg/m}^3$ in the crust increasing with depth to above 6×10^{17} or $8 \times 10^{17} \text{ kg/m}^3$ deeper inside[1].

In general, compact stars with less than 1.44 solar masses (the Chandrasekhar limit) are white dwarfs. Gravitational collapse will usually occur on any compact star above 10 solar masses and produce a black hole[2].

1.1.1 Formation of Neutron Stars

As the core of a massive star is compressed during a supernova explosion, and collapses into a neutron star, it retains most of its angular momentum. Since it has only a tiny

fraction of its parent's radius (and therefore its moment of inertia is sharply reduced), a neutron star is formed with very high rotation speed, and then gradually slows down. Neutron stars are known to have rotation periods between about 1.4 ms to 30 seconds. The neutron star's density also gives it very high surface gravity with typical values of a few $\times 10^{12} m/s^2$ (that is more than 10^{10} times that of Earth's). One measure of such immense gravity is the fact that neutron stars have gravity velocity of around $100,000 km/s$, about a third the speed of light. Matter falling onto the surface of a neutron star would be accelerated to tremendous speed by the star's gravity. The force of impact would likely destroy the object's component atoms, rendering all its matter identical, in most respects, to the rest of the star.

1.1.2 Structure of Neutron Stars

The interior structure of a neutron star consists of iron, neutron rich nuclei and electrons in the outer crystalline solid crust. The inner crust contains neutron rich nuclei, free superfluid neutrons and electrons and the interior, superfluid neutrons, superfluid protons and electrons. The makeup of the core is unknown. It is mystery how matter behaves at these amazingly high densities.

The outer layer of a neutron star has a complex structure which depends strongly on the nuclear density. If the surface temperature exceeds 10^6 kelvin (as in the case of a young neutron star), the surface should be fluid instead of the solid phase observed in cooler neutron stars (temperature $< 10^6$ kelvins)[4]. In the inner crust of the star, due to the high density and pressure, a large fraction of neutrons occupy unbound states.

The "atmosphere" of the star is roughly one meter thick, and its dynamic is fully controlled by the star's magnetic field. Below the atmosphere one encounters a solid "crust". This crust is extremely hard and very smooth (with maximum surface irregularities of 5 mm), because of the extreme gravitational field[5]. Proceeding inward, one encounters nuclei with ever increasing numbers of neutrons; such nuclei would decay quickly on

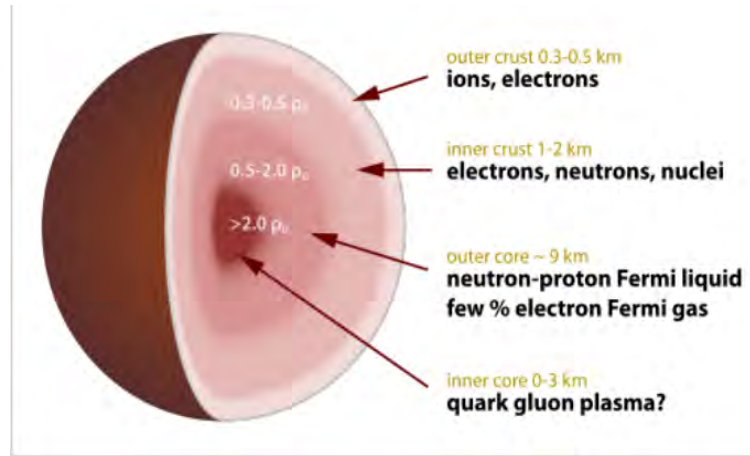


Figure 1.1: The stacture of neutron star

Earth, but are kept stable by tremendous pressures. Proceeding deeper, one comes to a point called neutron drip where neutrons leak out of nuclei and become free neutrons. In this region, there are nuclei, free electrons, and free neutrons. The nuclei become smaller and smaller until the core is reached, by definition the point where they disappear altogether. The composition of the superdense matter in the core remains uncertain. One model describes the core as superfluid neutron-degenerate matter (mostly neutrons, with some protons and electrons). More exotic forms of matter are possible, including degenerate strange matter (containing strange quarks in addition to up and down quarks), matter containing high-energy pions and kaons in addition to neutrons[2], or ultra-dense quark-degenerate matter.

1.1.3 Discoveries

In 1965, Antony Hewish and Samuel Okoye discovered "an unusual source of high radio brightness temperature in the Crab Nebula"[10]. This source turned out to be the Crab Nebula neutron star that resulted from the great supernova of 1054.

In 1967, Iosif Shklovsky examined the X-ray and optical observations of Scorpius X-1 and correctly concluded that the radiation comes from a neutron star at the stage of accretion[11].

In 1967, Jocelyn Bell and Antony Hewish discovered regular radio pulses from CP 1919. This pulsar was later interpreted as an isolated, rotating neutron star. The energy source of the pulsar is the rotational energy of the neutron star. The majority of known neutron stars (about 2000, as of 2010) have been discovered as pulsars, emitting regular radio pulses.

In 1971, Riccardo Giacconi, Herbert Gursky, Ed Kellogg, R. Levinson, E. Schreier, and H. Tananbaum discovered 4.8 second pulsations in an X-ray source in the constellation Centaurus, Cen X-3. They interpreted this as resulting from a rotating hot neutron star. The energy source is gravitational and results from a rain of gas falling onto the surface of the neutron star from a companion star or the interstellar medium.

In 1974, Joseph Taylor and Russell Hulse discovered the first binary pulsar, PSR B1913+16, which consists of two neutron stars (one seen as a pulsar) orbiting around their center of mass. Einstein's general theory of relativity predicts that massive objects in short binary orbits should emit gravitational waves, and thus that their orbit should decay with time. This was indeed observed, precisely as general relativity predicts, and in 1993, Taylor and Hulse were awarded the Nobel Prize in Physics for this discovery.

In 2010, Paul Demorest and colleagues measured the mass of the millisecond pulsar PSR J1614-2230 to be 1.97 ± 0.04 solar masses, using Shapiro delay[12]. This is substantially higher than any other precisely measured neutron star mass (in the range 1.2-1.45 solar masses), and places strong constraints on the interior composition of neutron stars.

1.1.4 Rotation

Neutron stars rotate extremely rapidly after their creation due to the conservation of angular momentum; like spinning ice skaters pulling in their arms, the slow rotation of the original star's core speeds up as it shrinks. A newborn neutron star can rotate several times a second; sometimes, the neutron star absorbs orbiting matter from a companion star, increasing the rotation to several hundred times per second, reshaping the neutron star into an oblate spheroid. Over time, neutron stars slow down because of their rotating magnetic fields radiate energy; older neutron stars may take several seconds for each revolution. The rate at which a neutron star slows its rotation is usually constant and very small:

1.1.5 Magnetic Field

Neutron stars contain persistent, ordered magnetic fields that are the strongest known in the Universe. Pulsars are very strongly magnetized rotating neutron stars. The flux being conserved, in the collapsing stellar material. Since the interior of the star is superfluid, the decay time is long compared with the life time of a pulsar. Polar field strengths reaching 10^{12} G occur in young pulsars; found in the main body of pulsars, while in the older evolved millisecond pulsars it is relatively as low as $10^9 G$. The active pulsars in the galaxy have surface magnetic fields in the range of $\sim 26 \times 10^{12} G$: This is still thousands of times larger than fields attainable in the laboratory. Despite the intensity of the magnetic field, it has very little effect on the structure of the star. Outside the star, however the magnetic field B completely dominates all physical processes, even outweighing gravitation by a very large factor.

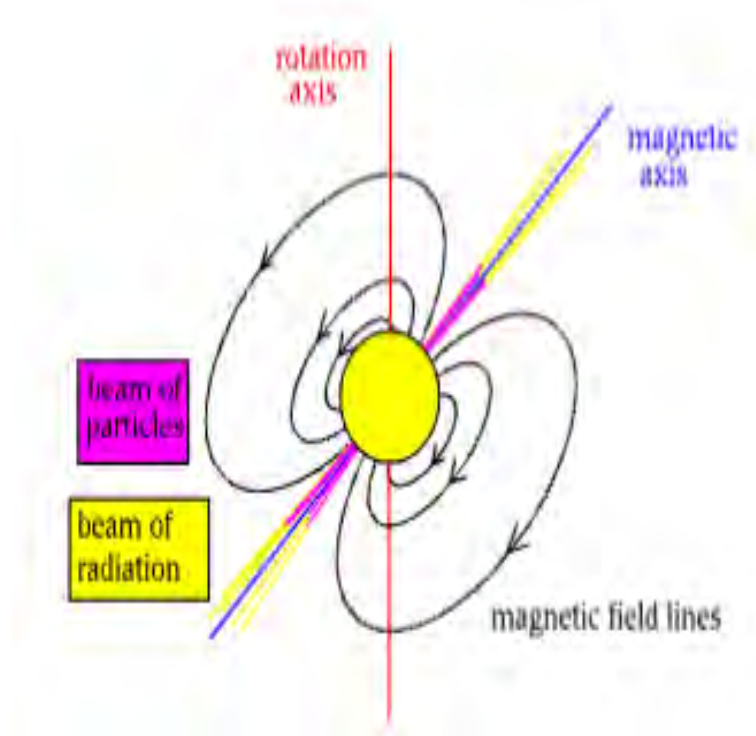


Figure 1.2: Pulsars rotation axis, magnetic axis, and magnetic field

1.1.6 Magnetic Field

The external magnetic field plays a crucial part in several observable characteristics of pulsars, which is our area of interest. The magnetic moment is substantially misaligned with the rotation axis and allows the pulsar to radiate, its rotational kinetic energy away. this accounts for the observed slow down. The radiation is expected to exert pressure on the inner radius of an accretion disk around a neutron star.

Lines of magnetic force will be carried along with the collapse of the plasma core of the star. As the core collapses the magnetic field lines are pulled more closely together, intensifying the magnetic field to values of the order of 10^{12} gauss, which leads to magnetic flux Conservation. Pulsars produce a Lighthouse Effect due to an intense magnetic field whose axis is misaligned with its rotational axis. One popular view is that the rapid rotation and intense magnetic field of the neutron star generates strong electric fields, which accelerate charged particles (principally electrons because they are less massive) near the magnetic poles where the magnetic field is most intense.

1.1.7 Conservation of Magnetic Field

Most stars are believed to generate a (roughly) dipole magnetic field due to churning motion of the conducting plasma in their interiors. When a dying star collapses to form a neutron star, magnetic flux conservation results in the formation of regions of extremely strong magnetic field near the neutron star.

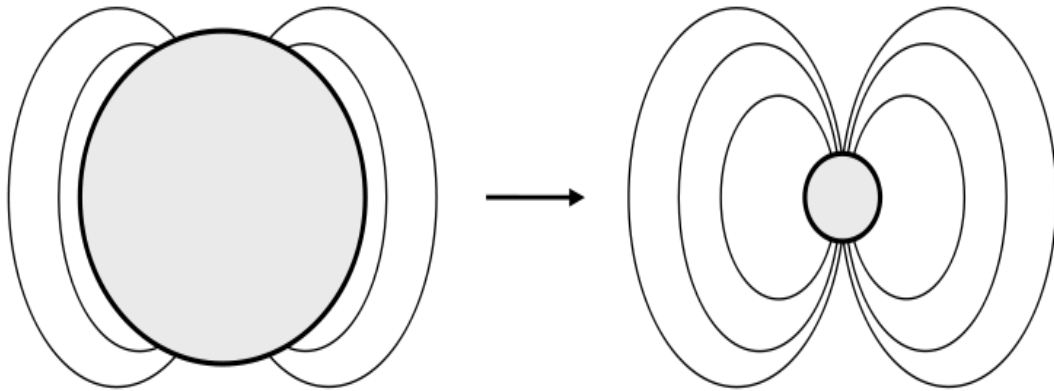


Figure 1.3: Magnetic flux conservation

As a result, the magnetic flux through a surface element is conserved. Pictorially, the total number of magnetic field lines running through the surface will remain unchanged, even if you adjust the size of the surface. The spacing of the field lines gives a measure of the strength of the field: closer field line spacing = stronger magnetic field.

Rotating neutron stars formed in a supernova explosion in which massive stars die explosively. In the process the residual magnetic field of the star gets conserved in the neutron star which is formed after the explosion. As a result the intensity of the magnetic field of the progenitor star will intensify inside the neutron star to a high level. We demonstrate this as follows; let us assume that the progenitor star is as big as our sun whose surface magnetic field is known to be $\sim 10^4 G$. The magnetic flux corresponding to this will be

$$\Phi_s = 4\pi r_s^2 \times 10^4 G cm^2 \quad (1.1.1)$$

where $r_s \approx 7 \times 10^5 \text{km} \approx 7 \times 10^{10} \text{cm}$ hence

$$\Phi_s = 4\pi \times (7 \times 10^{10})^2 \times 10^4 \text{Gcm}^2 \quad (1.1.2)$$

$$\Phi_s \approx 9 \times 10^{26} \text{Gcm}^2 \quad (1.1.3)$$

By the principle of flux conservation we expect

$$4\pi r_s^2 \times 10^4 = B_N * 4\pi r_N^2 \quad (1.1.4)$$

where \mathbf{B}_N is the surface magnetic field of the neutron star and r_N is the radius of the neutron star which known to be of the order $10 \text{km} = 10^6 \text{cm}$. Hence

$$\mathbf{B}_N = \frac{4\pi r_s^2 \times 10^4 \text{Gcm}^2}{4\pi r_N^2 \text{cm}^2} \quad (1.1.5)$$

$$= \frac{4\pi * 9 \times 10^{26} \text{Gcm}^2}{4\pi 10^{12} \text{cm}^2} \quad (1.1.6)$$

$$= 9 \times 10^{14} \text{G} \quad (1.1.7)$$

This shows a neutron star is strongly magnetized at birth. The magnetization vector associated with this magnetic field is usually an oblique rotator. Since \mathbf{m} is oblique the vector potential is rotated at any field is sinusoidal and hence time. This kind of neutron star is called a pulsar and it is supposed radiator.

Chapter 2

MAGNETIC FIELD LINE GEOMETRY

2.1 Expansion of Multipole Vector Potential

The vector potential at a given field point \mathbf{r} of rotating neutron star with a net surface charge different from zero, is given by

$$\mathbf{A}(\mathbf{r}) = \int_{v'} dv' \frac{\mathbf{J}(\mathbf{r}')}{|\mathbf{r} - \mathbf{r}'|} \quad (2.1.1)$$

where \mathbf{J} is the current density.

This can be rewritten in term of the legendre polynomials, which are defined by

$$|\mathbf{r} - \mathbf{r}'|^{-1} = \sum_l \frac{\mathbf{r}'^l}{\mathbf{r}^{l+1}} P_l(\cos \theta) \quad (2.1.2)$$

where θ is the angle between \mathbf{r} and \mathbf{r}'

Using the addition theorem for spherical harmonics, which expresses the legendre polynomials $P_l(\cos \theta)$ as the sum of the product of the spherical harmonics $Y_{lm}(\theta', \phi')$ and $Y_{lm}^*(\theta, \phi)$ over the range $m = -1, \dots, l$,

$$P_l(\cos \theta) = \frac{4\pi}{2l+1} \sum Y_{lm}^*(\theta, \phi) Y_{lm}(\theta', \phi') \quad (2.1.3)$$

where the spherical harmonic defined by

$$Y_{lm}(\theta, \phi) = (-1)^m \left(\frac{2l+1}{4\pi}\right)^{\frac{1}{2}} \left(\frac{(l-m)!}{(l+m)!}\right)^{\frac{1}{2}} P_m(\cos \theta) e^{im\phi} \quad (2.1.4)$$

Substituting these we can write the expansion as

$$|\mathbf{r} - \mathbf{r}'|^{-1} = \sum_{lm} \frac{r'^l}{r^{l+1}} Y_{lm}(\theta, \phi) Y_{lm}^*(\theta', \phi') \quad (2.1.5)$$

which make the vector potential to be written as

$$A(x) = \sum_{lm} \frac{4\pi}{2l+1} \int_{v'} \mathbf{J}(\mathbf{r}') \frac{r'^l}{r^{l+1}} Y_{lm}(\theta, \phi) Y_{lm}^*(\theta', \phi') dv' \quad (2.1.6)$$

where $\mathbf{r}_< \rightarrow \mathbf{r} < \mathbf{r}'$ and $\mathbf{r}_> \rightarrow \mathbf{r} > \mathbf{r}'$

In a uniform spherical charge distribution with surface charge density σ ,

$$\sigma = \frac{|Q|}{4\pi R^2} \quad (2.1.7)$$

the current density in the system is given by

$$\mathbf{J} = \sigma \delta(\mathbf{r}' - R) v \quad (2.1.8)$$

$$\mathbf{J} = \sigma \delta(\mathbf{r}' - R) \vec{w} \times \mathbf{r}$$

where

$$\vec{w} \times \mathbf{r} = \begin{pmatrix} \hat{x} & \check{y} & \hat{z} \\ 0 & 0 & w \\ R \sin \theta \cos \phi' & R \sin \theta' \sin \phi' & R \cos \theta' \end{pmatrix} \quad (2.1.9)$$

In Cartesian components

$$\vec{w} \times \mathbf{r} = -Rw \sin \theta' \sin \phi' \hat{x} + Rw \sin \theta' \cos \phi' \hat{y} \quad (2.1.10)$$

or in spherical polar coordinates

$$\vec{w} \times \mathbf{r} = Rw \sin \theta' \hat{e}'_{\phi} \quad (2.1.11)$$

where,

$$\hat{e}'_{\phi} = -\sin \phi' \hat{x} + \cos \phi' \hat{y}$$

Therefore, the vectorial current density \mathbf{J} can be written

$$\mathbf{J} = -\mathbf{J}_{\phi} \sin \phi' \hat{x} + \mathbf{J}_{\phi} \cos \phi' \hat{y} \quad (2.1.12)$$

since the geometry is spherical symmetric, we may choose for simplicity; the observation point on the xz-plane ($\phi' = 0$). The azimuthal integration in equation (2.1.14) is symmetric about $\phi' = 0$, terms have no contribution. This leaves only the y component, which is A_ϕ . Thus

$$\int_0^{2\pi} \cos \phi' d\phi' = \int_0^{2\pi} \sin \phi' d\phi' = 0 \quad (2.1.13)$$

the vector potential will be

$$\mathbf{A}(\mathbf{x}) = \frac{Rw|Q|}{4\pi R^2} \sum_{lm} \frac{4\pi}{2l+1} \int_{v'} \delta(\mathbf{r}' - R) \frac{\mathbf{r}'_{<}}{r_{>}^{l+1}} Y_{lm}(\theta, \phi) Y_{lm}^*(\theta', \phi') \cos \phi' \sin \theta' \mathbf{r}'^2 dr' d\Omega' \quad (2.1.14)$$

The solid angle $d\Omega' = \sin \theta' d\theta' d\phi'$

$$\begin{aligned} \mathbf{A}(\mathbf{x}) = & \frac{Rw|Q|}{4\pi R^2} \sum_{lm} \frac{4\pi}{2l+1} Y_{lm}(\theta, \phi) \int_0^{2\pi} \int_0^\pi \int_0^\infty \delta(\mathbf{r}' - R) \frac{\mathbf{r}'_{<}}{r_{>}^{l+1}} \\ & * Y_{lm}^*(\theta', \phi') \cos \phi' \sin^2 \theta' \mathbf{r}'^2 dr' d\theta' d\phi' \end{aligned} \quad (2.1.15)$$

The Vector potential everywhere outside of the neutron star will be obtained by substituting $\mathbf{r}_{<} = R$ and $r_{>} = r$ we get

$$\begin{aligned} \mathbf{A}_{\phi, out} = & \frac{Rw|Q|}{4\pi R^2} \sum_{lm} \frac{4\pi}{2l+1} \frac{R^l}{r^{l+1}} Y_{l,m}(\theta, \phi) \\ & * \int_0^{2\pi} \int_0^\pi \int_0^\infty Y_{lm}^*(\theta', \phi') \delta(\mathbf{r}' - R) \cos \phi' \sin^2 \theta' \mathbf{r}'^2 dr' d\theta' d\phi' \end{aligned} \quad (2.1.16)$$

2.2 Dipole Vector Potential

From the above general multipole expansion we will drive for specific case to the dipole vector potential by substitute the value of l is one

$$\begin{aligned} \mathbf{A}_{\phi, out} = & \frac{Rw|Q|}{4\pi R^2} \sum_{lm} \frac{4\pi}{3} \frac{R}{r^2} Y_{l,m}(\theta, \phi) \\ & * \int_0^{2\pi} \int_0^\pi \int_0^\infty Y_{lm}^*(\theta', \phi') \delta(\mathbf{r}' - R) \cos \phi' \sin^2 \theta' \mathbf{r}'^2 dr' d\theta' d\phi' \end{aligned} \quad (2.2.1)$$

Integration over the delta function becomes

$$\int \delta(\mathbf{r}' - R)r'^2 dr' = R^2 \quad (2.2.2)$$

The vector potential will have the relation

$$\begin{aligned} \mathbf{A}_{\phi,out} &= \frac{R^3 w |Q|}{4\pi R^2} \sum_{lm} \frac{4\pi}{3} \frac{R}{r^2} Y_{l,m}(\theta, \phi) \\ * \int_0^{2\pi} \int_0^\pi Y_{lm}^*(\theta', \phi') \cos \phi' \sin^2 \theta' d\theta' d\phi' \end{aligned} \quad (2.2.3)$$

Taking the spherical harmonic value

$$Y_{11}^*(\theta, \phi) = -\sqrt{\frac{3}{8\pi}} \sin \theta e^{i\phi} \quad (2.2.4)$$

The potential will be

$$\begin{aligned} \mathbf{A}_{\phi,out} &= \frac{R^3 w |Q|}{4\pi R^2} \sum_{lm} \frac{4\pi}{3} \frac{R}{r^2} Y_{l,m}(\theta, \phi) \\ * \int_0^{2\pi} \int_0^\pi \left(-\sqrt{\frac{3}{8\pi}} \sin^3 \theta e^{i\phi} \right) \cos \phi' d\theta' d\phi' \end{aligned} \quad (2.2.5)$$

The integral with $d\phi'$ will become

$$\int e^{i\phi} \cos \theta' d\phi' = \pi \quad (2.2.6)$$

The vector potential will the form

$$\begin{aligned} \mathbf{A}_{\phi,out} &= \frac{R^3 w \pi |Q|}{4\pi R^2} \sum_{lm} \frac{4\pi}{3} \frac{R}{r^2} Y_{l,m}(\theta, \phi) \\ * \int_0^{2\pi} \int_0^\pi \left(-\sqrt{\frac{3}{8\pi}} \sin^3 \theta \right) d\theta' \end{aligned} \quad (2.2.7)$$

The integral with $d\theta'$ will become

$$\int_0^\pi \sin^3 \theta' d\theta' = \frac{4}{3} \quad (2.2.8)$$

and hence will make the potential to be

$$\mathbf{A}_{\phi,out} = \frac{R^3 w \pi |Q|}{4\pi R^2} \frac{4}{3} \sum_{lm} \frac{4\pi}{3} \frac{4\pi}{3} Y_{l,m}(\theta, \phi) \left(-\sqrt{\frac{3}{8\pi}} \right) \quad (2.2.9)$$

But the spherical harmonic for unprimed term is

$$Y_{11}(\theta, \phi) = -\sqrt{\frac{3}{8\pi}} \sin \theta e^{i\phi} \quad (2.2.10)$$

We have then obtain the vector potential as

$$\mathbf{A}_{\phi, out} = \frac{R^3 w \pi |Q|}{4\pi R^2} \frac{4}{3} \frac{R}{r^2} \sum_{lm} \frac{4\pi}{3} Y_{l,m}(\theta, \phi) \left(\sqrt{\frac{3}{8\pi}} \right) \left(\sqrt{\frac{3}{8\pi}} \sin \theta e^{i\phi} \right) \quad (2.2.11)$$

Focusing only on the magnitude

$$\mathbf{A}_{\phi, out} = \frac{R^3 w \pi |Q|}{4\pi R^2} \frac{4}{3} \frac{R}{r^2} \sum_{lm} \frac{4\pi}{3} Y_{l,m}(\theta, \phi) \left(\sqrt{\frac{3}{8\pi}} \right) \left(\sqrt{\frac{3}{8\pi}} \sin \theta \right) \quad (2.2.12)$$

finally the vector potential can be written as

$$\mathbf{A}_{\phi, out} = \frac{|Q| w R^2}{3r^2} \sin \theta \quad (2.2.13)$$

2.3 Derivation of Magnetic Field

In basic differential laws of magnetostatics, we see that due to the absence of free magnetic monopoles (charges) the divergence of the magnetic field \mathbf{B} vanishes. Therefore, \mathbf{B} must be the curl of some vector field $\mathbf{A}(\mathbf{r})$, called the vector potential[8]. Hence, we can write as

$$\mathbf{B} = \nabla \times \mathbf{A} \quad (2.3.1)$$

which can be written as spherical coordinate

$$\begin{aligned} \vec{\nabla} \times \vec{\mathbf{A}} &= \frac{1}{r \sin \theta} \left[\frac{\partial}{\partial \theta} (\mathbf{A}_\phi \sin \theta) - \frac{\partial}{\partial \phi} \mathbf{A}_\theta \right] \hat{e}_r \\ &+ \left[\frac{1}{r \sin \theta} \frac{\partial \mathbf{A}_r}{\partial \phi} - \frac{1}{r} \frac{\partial}{\partial r} (r \mathbf{A}_\phi) \right] \hat{e}_\theta \\ &+ \frac{1}{r} \left[\frac{\partial}{\partial r} (r \mathbf{A}_\theta) - \frac{\partial \mathbf{A}_r}{\partial \theta} \right] \hat{e}_\phi \end{aligned} \quad (2.3.2)$$

But we have only the ϕ component of the vector potential. The magnetic field will be

$$\mathbf{B} = \frac{1}{r \sin \theta} \left[\frac{\partial}{\partial \theta} (\sin \theta \mathbf{A}_\phi) \right] \hat{e}_r - \frac{1}{r} \frac{\partial}{\partial r} (r \mathbf{A}_\phi) \hat{e}_\theta \quad (2.3.3)$$

In component form;

$$\mathbf{B}_r = \frac{1}{r \sin \theta} \left[\frac{\partial}{\partial \theta} (\sin \theta \mathbf{A}_\phi) \right] \hat{e}_r \quad (2.3.4)$$

$$\mathbf{B}_\theta = -\frac{1}{r} \frac{\partial}{\partial r} (r \mathbf{A}_\phi) \hat{e}_\theta \quad (2.3.5)$$

$$\mathbf{B}_\phi = 0 \quad (2.3.6)$$

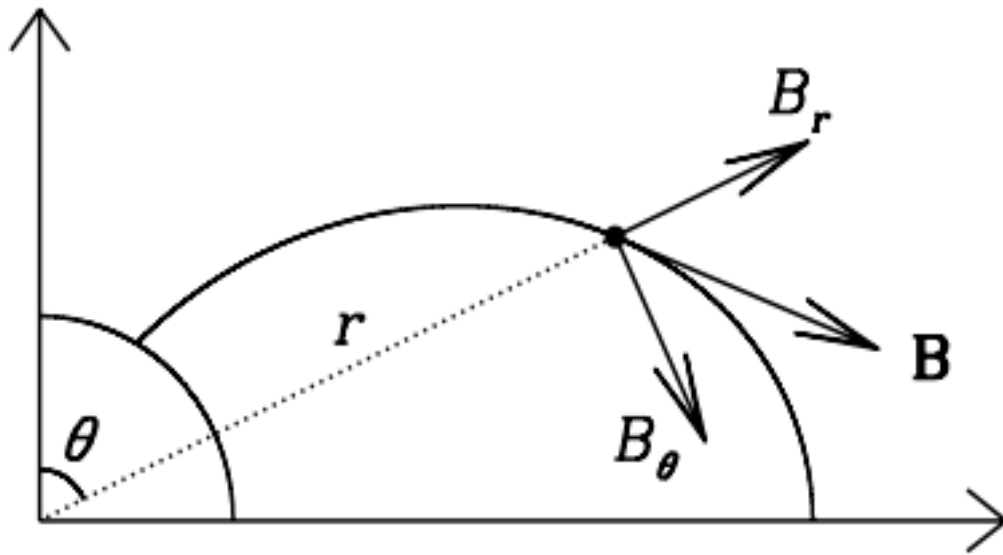


Figure 2.1: Shows a field vector \mathbf{B} decomposed into the radial \mathbf{B}_r and polar \mathbf{B}_θ components

2.4 Magnetic Field Outside The Crust

The magnetic field outside the crust can be calculated as

$$\mathbf{B}_{out} = \nabla \times \mathbf{A}_{out} \quad (2.4.1)$$

$$\begin{aligned} \mathbf{B}_{out} &= \frac{1}{r \sin \theta} \left[\frac{\partial}{\partial \theta} (\sin \theta \mathbf{A}_{\phi, out}) \right] \hat{e}_r - \frac{1}{r} \frac{\partial (r \mathbf{A}_{\phi, out})}{\partial r} \hat{e}_\theta \\ \mathbf{B}_{out} &= \left[\frac{\cos \theta \mathbf{A}_{\phi, out}}{r \sin \theta} + \frac{1}{r} \frac{\partial \mathbf{A}_{\phi, out}}{\partial \theta} \right] \hat{e}_r - \left[\frac{\mathbf{A}_{\phi, out}}{r} + \frac{\partial \mathbf{A}_{\phi, out}}{\partial r} \right] \hat{e}_\theta \end{aligned}$$

Recalling the vector potential outside the star

$$\begin{aligned} \mathbf{B}_{out} &= \frac{|Q|wR^2}{3} \left[\frac{\cos \theta}{r^3} + \frac{1}{r^3} \frac{\partial \sin \theta}{\partial \theta} \right] \hat{e}_r \\ &\quad - \frac{|Q|wR^2}{3} \left[\frac{\sin \theta}{r^3} + \frac{\partial}{\partial r} \left(\frac{\sin \theta}{r^2} \right) \right] \hat{e}_\theta \end{aligned}$$

we obtain

$$\mathbf{B}_{out} = \frac{|Q|wR^2}{3r^3} (2 \cos \theta \hat{e}_r + \sin \theta \hat{e}_\theta) \quad (2.4.2)$$

Therefore, the component of the dipole magnetic field

$$\mathbf{B}_r = \frac{2|Q|wR^2}{3r^3} \cos \theta \quad (2.4.3)$$

and

$$\mathbf{B}_\theta = \frac{|Q|wR^2}{3r^3} \sin \theta \quad (2.4.4)$$

When we consider the maximum intensity of the radial part of the dipolar magnetic field,

$$\mathbf{B}_r = \frac{2|Q|wR^2}{3r^3} \quad (2.4.5)$$

But we assume that the magnitude of magnetic field that we have derived from the magnetic flux conservation is dominated by dipolar, so we can relate the dipolar magnetic field that we have derived in equation (2.3.9) with magnetic flux conservation in chapter one which is given by

$$\mathbf{B}_N = 9 \times 10^{14} G \quad (2.4.6)$$

now we can make the approximation of the two terms will lead to

$$9 \times 10^{14} G \approx \frac{2|Q|wR^2}{3r^3} \quad (2.4.7)$$

Take another assumption that the field point is settled around the surface of the neutron star, this lead to make an approximation $r \approx R$, then the above equation will be

$$9 \times 10^{14} G \approx \frac{2|Q|wR^2}{3R^3} \quad (2.4.8)$$

$$9 \times 10^{14} G \approx \frac{2|Q|w}{3R} \quad (2.4.9)$$

But hear in the equation we know the magnitude of the radius of neutron star $R \approx 10km \approx 10^6cm$, substitute this we get the relation of charge with angular frequency of the neutron star;

$$13.5 \times 10^{20} Gcm \approx Qw \quad (2.4.10)$$

Substituting this value in to equation (2.3.9) we get the radial part of the dipole magnetic field as

$$\mathbf{B}_r = 2 \frac{(13.5 \times 10^{20} GcmR^2)}{3r^3} \cos \theta \quad (2.4.11)$$

This approximation may lead to estimate the magnetic dipole moment to be

$$\mathbf{m} = QwR^2 \quad (2.4.12)$$

The magnetic dipole moment approximate to

$$\mathbf{m} \approx 9 \times 10^{32} Gcm^2 \quad (2.4.13)$$

and also the angular component of magnetic dipole will be

$$\mathbf{B}_\theta = \frac{13.5 \times 10^{20} GcmR^2}{3r^3} \sin \theta \quad (2.4.14)$$

2.5 Magnetic Field Line

A simpler way to visualize the magnetic field is to 'connect' the arrows to form "magnetic field lines". Magnetic field lines make it much easier to visualize and understand the complex mathematical relationships underlying magnetic field. If done carefully, a field line diagram contains the same information as the vector field it represents. The magnetic field can be estimated at any point on a magnetic field line diagram (whether on a field line or not) using the direction and density of nearby magnetic field lines. A higher density of nearby field lines indicates a stronger magnetic field.

2.6 Dipole Magnetic Field Line

Since an element of a line of magnetic field, having component of dr and $d\theta$, is parallel to the the local \mathbf{B} , whose components are \mathbf{B}_r and \mathbf{B}_θ , and the component differential element are given

$$dr = dr\hat{r} + rd\theta\hat{\theta} + r\sin\theta d\phi\hat{\phi} \quad (2.6.1)$$

$$\vec{\mathbf{B}} = B_r\hat{r} + B_\theta\hat{\theta} + 0\hat{\phi} \quad (2.6.2)$$

Dividing the correspondence terms of the above two equations we will get

$$\frac{dr}{\mathbf{B}_r} = \frac{rd\theta}{\mathbf{B}_\theta} = \beta \quad (2.6.3)$$

where β is a constant related to curvature, rearrange above equation

$$\frac{dr}{rd\theta} = \frac{\mathbf{B}_r}{\mathbf{B}_\theta} \quad (2.6.4)$$

Substituting equation (2.3.17) and equation (2.3.18) in to the above equation and canceling similar terms

$$\frac{dr}{rd\theta} = \frac{2\cos\theta}{\sin\theta} \quad (2.6.5)$$

which implies

$$\frac{dr}{rd\theta} = 2\cot\theta \quad (2.6.6)$$

Integrating this equation

$$\int \frac{dr}{r} = \int 2 \cot \theta d\theta \quad (2.6.7)$$

which is equal to

$$\ln r = 2 \ln(\sin \theta) + \ln K_d \quad (2.6.8)$$

$$= \ln(\sin \theta)^2 + \ln K_d \quad (2.6.9)$$

$$r = K_d \sin^2 \theta \quad (2.6.10)$$

This equation can determines the line of magnetic field for magnetic dipole as shown below.

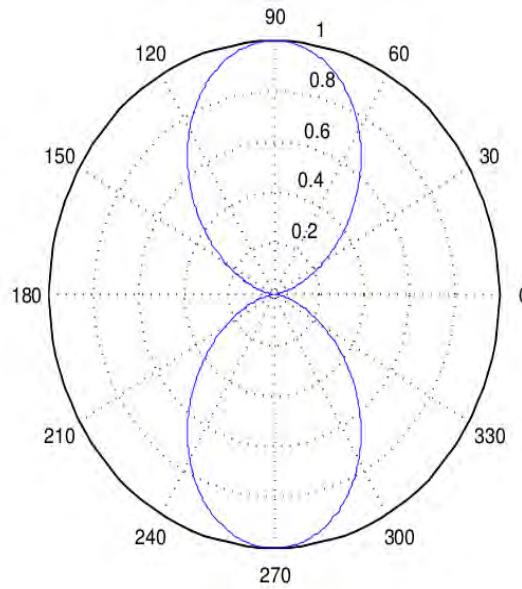


Figure 2.2: The geometry of field lines from magnetic dipole moment when $K_d = 1$

The constant K_d is a parameter that varies one line of the field to the another. This graph shows that the dipolar field line is maximum at the poles and the dipolar magnetic field line is minimum at the equatorial ring.

2.7 Quadrupole Vector Potential

We can derive the magnetic field for the quadrupole term by using the general multipole expansion in equation (2.1.16) with the value of l equal to two that leads to be the

vector potential to have the form

$$\begin{aligned} \mathbf{A}_{\phi,out} &= \frac{Rw|Q|}{4\pi R^2} \sum_{lm} \frac{4\pi R^2}{5 r^3} Y_{l,m}(\theta, \phi) \\ &* \int_0^{2\pi} \int_0^\pi \int_0^\infty Y_{lm}^*(\theta', \phi') \delta(\mathbf{r}' - R) \cos \phi' \sin^2 \theta' \mathbf{r}'^2 dr' d\theta' d\phi' \end{aligned} \quad (2.7.1)$$

The integration over a delta function will become

$$\int \delta(\mathbf{r}' - R) r'^2 dr' = R^2 \quad (2.7.2)$$

That makes the vector potential to be

$$\begin{aligned} \mathbf{A}_{\phi,out} &= \frac{R^3 w |Q|}{4\pi R^2} \sum_{lm} \frac{4\pi R^2}{5 r^3} Y_{l,m}(\theta, \phi) \\ &* \int_0^{2\pi} \int_0^\pi \int_0^\infty Y_{lm}^*(\theta', \phi') \cos \phi' \sin^2 \theta' d\theta' d\phi' \end{aligned} \quad (2.7.3)$$

The spherical harmonic for quadrupole will have the relation

$$Y_{21}^*(\theta', \phi') = -\sqrt{\frac{15}{8\pi}} \cos \theta' \sin \theta' e^{i\phi'} \quad (2.7.4)$$

and inserting this in to equation the vector potential

$$\begin{aligned} \mathbf{A}_{\phi,out} &= \frac{R^3 w |Q|}{4\pi R^2} \sum_{lm} \frac{4\pi R^2}{5 r^3} Y_{l,m}(\theta, \phi) \\ &* \int_0^{2\pi} \int_0^\pi \int_0^\infty \left(-\sqrt{\frac{15}{8\pi}} \cos \theta' \sin \theta' e^{i\phi'} \right) \cos \phi' \sin^2 \theta' d\theta' d\phi' \end{aligned} \quad (2.7.5)$$

The integration over the angle ϕ

$$\int_0^{2\pi} \cos \phi' e^{i\phi'} d\phi' = \pi \quad (2.7.6)$$

The integration over the angle θ became

$$\int_0^\pi \sin^3 \theta' \cos \theta' d\theta' = 1 \quad (2.7.7)$$

then substituting the above two equation in to equation (2.4.15) the vector potential

became

$$\mathbf{A}_{\phi,out} = \frac{R^3 w \pi |Q|}{4\pi R^2} \sum_{lm} \frac{4\pi R^2}{5 r^3} Y_{l,m}(\theta, \phi) \left(-\sqrt{\frac{15}{8\pi}} \right) \quad (2.7.8)$$

Again the spherical harmonic value for unprimed term is

$$Y_{21}(\theta, \phi) = -\sqrt{\frac{15}{8\pi}} \cos \theta \sin \theta e^{i\phi} \quad (2.7.9)$$

The vector potential for quadrupole term is then given by

$$\mathbf{A}_{\phi, out} = \frac{R^3 w \pi |Q|}{4\pi R^2} \sum_{lm} \frac{4\pi R^2}{5 r^3} \left(-\sqrt{\frac{15}{8\pi}} \right) \left(-\sqrt{\frac{15}{8\pi}} \cos \theta \sin \theta e^{i\phi} \right) \quad (2.7.10)$$

When we take the magnitude of the above equation

$$\mathbf{A}_{\phi, out} = \frac{R^3 w \pi |Q|}{4\pi R^2} \sum_{lm} \frac{4\pi R^2}{5 r^3} \left(-\sqrt{\frac{15}{8\pi}} \right) \left(-\sqrt{\frac{15}{8\pi}} \cos \theta \sin \theta \right) \quad (2.7.11)$$

finally we find the vector potential of quadrupole out side of the neutron star to be

$$\mathbf{A}_{\phi, out} = \frac{3R^3 w |Q|}{4r^3} \cos \theta \sin \theta \quad (2.7.12)$$

2.8 Quadrupole Magnetic Field

The quadrupole magnetic field can be calculated similar to that of the dipole term. The magnetic field outside the crust can be calculated as

$$\mathbf{B}_{out} = \nabla \times \mathbf{A}_{out} \quad (2.8.1)$$

$$\mathbf{B}_{out} = \frac{1}{r \sin \theta} \left[\frac{\partial}{\partial \theta} (\sin \theta \mathbf{A}_{\phi, out}) \right] \hat{e}_r - \frac{1}{r} \frac{\partial (r \mathbf{A}_{\phi, out})}{\partial r} \hat{e}_\theta$$

Recalling the vector potential out side of the neutron star

$$\begin{aligned} \mathbf{B}_{out} = \frac{3R^3 w |Q|}{4} \left[\frac{1}{r \sin \theta} \left(\frac{2 \sin \theta \cos^2 \theta - \cos \theta \sin^2 \theta}{r^3} \right) \right] \hat{e}_r \\ - \frac{3R^3 w |Q|}{4} \left[\frac{1}{r} \left(\frac{2 \sin \theta \cos \theta}{r^3} \right) \right] \hat{e}_\theta \end{aligned}$$

we obtain

$$\mathbf{B}_{out} = \frac{3R^3 w |Q|}{4} \left(\frac{(3 \cos^2 \theta - 1)}{r^4} \hat{e}_r + \frac{2 \sin \theta \cos \theta}{r^4} \hat{e}_\theta \right) \quad (2.8.2)$$

Therefore, the component of the dipole magnetic field are

$$\mathbf{B}_r = \frac{3R^3 w |Q|}{4r^4} (3 \cos^2 \theta - 1) \quad (2.8.3)$$

and

$$\mathbf{B}_\theta = \frac{3R^3 w |Q|}{2r^4} \sin \theta \cos \theta \quad (2.8.4)$$

Let us make some approximation for quadrupole cases similar to that of the dipole term, substitute equation (2.3.16) into the components of the quadrupole magnetic field

$$\mathbf{B}_r = \frac{3R^3 13.5 \times 10^{20} Gcm}{4r^4} (3 \cos^2 \theta - 1) \quad (2.8.5)$$

and the angular component of the quadrupole term will be

$$\mathbf{B}_\theta = \frac{3R^3 13.5 \times 10^{20} Gcm}{2r^4} \sin \theta \cos \theta \quad (2.8.6)$$

2.9 Quadrupole Magnetic Field line

To show the diagram of the magnetic field line of quadrupole term we have to know field line equation, so the field line equation can be calculated in a similar manner as we have done in case of dipole. We have derived the components of quadrupole fields in equation (2.4.27) and equation (2.4.28) and by substituting in equation (2.4.3) we get the following term

$$\frac{dr}{r} = \frac{\frac{3R^3 13.5 \times 10^{20} Gcm}{4r^4} (3 \cos^2 \theta - 1)}{\frac{3R^3 13.5 \times 10^{20} Gcm}{4r^4} \cos \theta \sin \theta} d\theta \quad (2.9.1)$$

$$\frac{dr}{r} = \frac{3 \cos^2 \theta - 1}{2 \sin \theta \cos \theta} d\theta \quad (2.9.2)$$

$$\frac{dr}{r} = \frac{1}{2} \int \frac{\cos \theta}{\sin \theta} + \int \cot 2\theta d\theta \quad (2.9.3)$$

Applying integration by substitution the above equation becomes

$$\ln r = \frac{1}{2} \ln(\sin \theta) + \frac{1}{2} \ln(\sin 2\theta) + \ln(K_Q) \quad (2.9.4)$$

where, K_Q integration constant for quadrupole term.

Applying the property of natural logarithm and simple rearrangement. The quadrupole magnetic field line parameter r can be calculated.

$$r = K_Q \sqrt{(\sin \theta \sin 2\theta)} \quad (2.9.5)$$

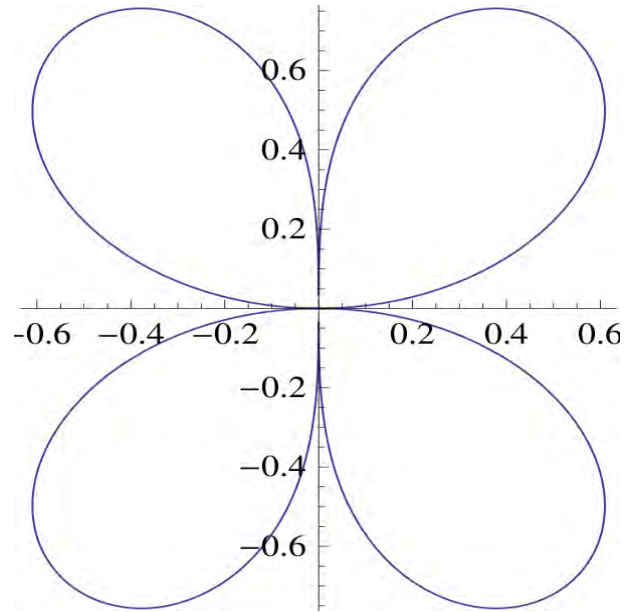


Figure 2.3: The geometry of the quadrupole field line where $K_Q = 1$

This graph indicates that the the quadrupole field line along the polar axis and along the equator of the ring is zero but when we make the angle varies between 0 and 90 degree the field attend maximum point. In addition the quadrupole magnetic field line in Fig (2.3) has four loops that is different as we compared with the two loop in the case of dipole field line.

Chapter 3

MAGNETIC RADIATION

In this chapter we shall be concerned with the ultimate source of all electromagnetic radiation of moving charge. We shall find that radiation can be produce only if a charge undergoes acceleration. The arbitrary motion of a collection of charges will produce radiation which can be describe a multi pole expansion. There is electric and magnetic multi pole radiation of all order. Here our attention is focused on specially magnetic dipole radiation and magnetic quadrapole radiation. Electro magnetic radiation has both electric and magnetic field components, which oscillate in phase perpendicular to each other and perpendicular to the direction of energy propagation.

3.1 The Retarded Potential For An Oscillating Magnetic Dipole

We consider a circular loop of radius a , lying in the x-y plane centered at the origin and carrying alternative current. As shown in Fig. (3.1) The current density \mathbf{J} has only a component in ϕ direction, by hypothesis, there is zero net charge and $V = 0$, We now have that

$$\mathbf{A} = \frac{\mu_0}{4\pi} \int_0^{2\pi} \frac{I e^{iw(t-r'/c)}}{r'} a \cos \phi d\phi \hat{\phi} \quad (3.1.1)$$

$$\mathbf{A} = \frac{\mu_0}{4\pi} a I e^{iw[t]} \int_0^{2\pi} \frac{expi(r-r')/\lambda'}{r'} \cos \phi d\phi \hat{\phi} \quad (3.1.2)$$

$$\frac{1}{r'} = \frac{1}{r} \left\{ 1 + \frac{a^2}{2r^2} + \frac{ax \cos \phi}{r^2} \right\} \quad (3.1.3)$$

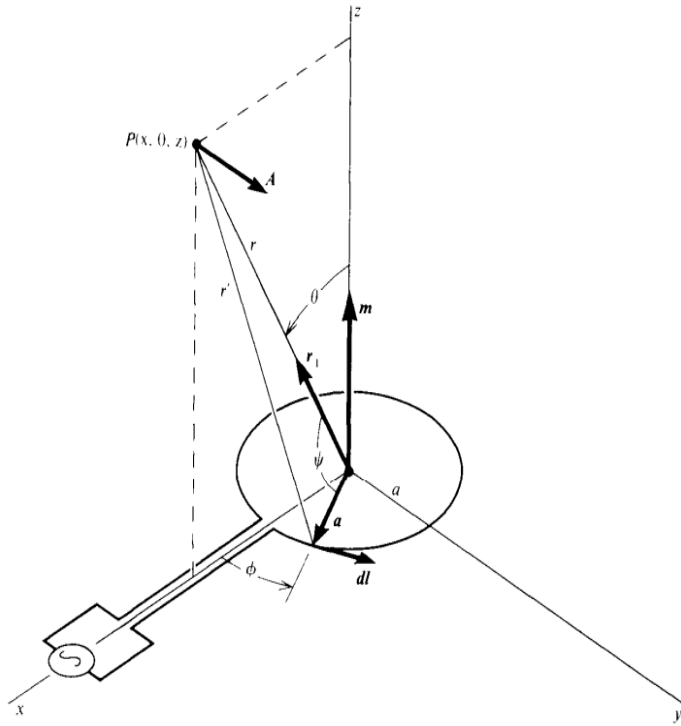


Figure 3.1: An oscillating magnetic dipole.

Then ,within the same approximation $R^3 \gg a^3$,

$$r' \approx r \left\{ 1 + \frac{a^2}{2r^2} - \frac{ax \cos \phi}{r^2} \right\}, \quad (3.1.4)$$

$$r - r' \approx \frac{ax \cos \phi}{r} - \frac{a^2}{2r} \quad (3.1.5)$$

also,

$$e^{i\frac{r-r'}{\lambda'}} \approx 1 + i\frac{r-r'}{\lambda'} \approx 1 + i\frac{ax \cos \phi}{r\lambda'} - i\frac{a^2}{2r\lambda'} \quad (3.1.6)$$

If $a^2 \ll 2\lambda'^2$.

Then the above integral in equation (3.1.2) becomes equal to

$$\frac{1}{r} \int_0^{2\pi} \left\{ 1 - \frac{a^2}{2r^2} + \frac{ax \cos \phi}{r^2} \right\} \left\{ 1 + i\frac{ax \cos \phi}{r\lambda'} - i\frac{a^2}{2r\lambda'} \right\} \cos \phi d\phi \quad (3.1.7)$$

This integral is easy to evaluate. First we disregard the $\cos^3 \theta$ terms because their integrals are zero. Also, the integral of $\cos^2 \phi$ is π .

Then the integral in (3.1.2) is equal to

$$\frac{\pi a x}{r^2} \left(\frac{1}{r} + i \frac{1}{\lambda'} \right) \quad (3.1.8)$$

Substituting now $r \sin \theta$ for x , and m for $\pi a^2 I$, m being the maximum value of the dipole moment, $\mathbf{m} = \mathbf{m}_0 e^{i\omega t}$

$$A = \frac{\mu_0 \mathbf{m}_0}{4\pi \lambda' r} \left(\frac{\lambda'}{r} + i \right) \sin \theta e^{i\omega(t - \frac{r}{c})} \hat{\phi} \quad (3.1.9)$$

$$A = \frac{i\mu_0 [\mathbf{m}] \times \hat{r}}{4\pi \lambda' r} \left(1 - i \frac{\lambda'}{r} \right) \quad (a^3 \ll r^3, a^2 \ll 2\lambda'^2) \quad (3.1.10)$$

For $r \gg \lambda'$ the vector potential propagates as a spherical wave of wave length whose amplitude is inversly propotional to r . However, \mathbf{A} is zero on the axis of symmetry and maximum on the equatorial plane.

3.2 Magnetic Dipole Radiation

In this section we will derive the time dependent magnetic field of the dipole component of the neutron star.

The magnetic field can be derived from vector potential as

$$\mathbf{B} = \nabla \times \mathbf{A} \quad (3.2.1)$$

$$\mathbf{B} = \frac{i\mathbf{m}_0 \mu_0}{4\pi \lambda'} \nabla \times \left\{ \frac{1}{r} \left(1 - i \frac{\lambda'}{r} \right) \sin \theta e^{i\omega(t - \frac{r}{c})} \hat{\phi} \right\} \quad (3.2.2)$$

$$\mathbf{B} = \frac{[\mathbf{m}] \mu_0}{4\pi \lambda'^2 r} \left\{ 2 \left(\frac{\lambda'^2}{r^2} + i \frac{\lambda'}{r} \right) \cos \theta \hat{r} + \left(-1 + \frac{\lambda'}{r^2} + i \frac{\lambda'}{r} \right) \sin \theta \hat{\theta} \right\} \quad (3.2.3)$$

At zero frequency, $\lambda' \rightarrow \infty$ and

$$\mathbf{B} = \frac{m}{4\pi r^3} (2 \cos \theta \hat{r} + \sin \theta \hat{\theta}) \quad (w = 0) \quad (3.2.4)$$

for $r \gg \lambda'$

$$\mathbf{B} = \frac{[m]}{4\pi \lambda'^2 r} \sin \theta \hat{\theta} \quad (r \gg \lambda') \quad (3.2.5)$$

since $V = 0$, and $w = c/\lambda'$

$$\mathbf{E} = -\frac{\partial \mathbf{A}}{\partial t} \quad (3.2.6)$$

$$\mathbf{E} = -i\omega\mathbf{A} \quad (3.2.7)$$

$$\mathbf{E} = \frac{\mu_0 c[\mathbf{m}]}{4\pi\lambda'^2 r} \left(1 - i\frac{\lambda'}{r}\right) \sin\theta\hat{\phi} \quad (3.2.8)$$

where $\mu_0 c \approx 337$ ohms. Thus \mathbf{E} is azimuthal.

At zero frequency, λ' is infinite and \mathbf{E} is zero, as expected.

For $r \gg \lambda'$,

$$\mathbf{E} = \frac{\mu_0 c[\mathbf{m}]}{4\pi\lambda'^2 r} \sin\theta\hat{\phi} \quad (3.2.9)$$

Observe that \mathbf{E} is proportional to the time derivative of \mathbf{A} ,

3.3 Poynting Vector

The Poynting vector can be thought of as representing the energy flux in (W/m^2) of an electromagnetic field. It is named after its inventor John Henry Poynting. The Poynting vector represents the particular case of an energy flux vector for electromagnetic energy. However, any type of energy has its direction of movement in space, as well as its density, so energy flux vectors can be defined for other types of energy as well. For time-harmonic electromagnetic fields, the average power flow over time can be found as follows,

$$\langle s \rangle = \frac{1}{2} \text{Re}(\mathbf{E} \times \mathbf{B}^*) \quad (3.3.1)$$

$$\langle s \rangle = \frac{1}{2} \left\{ \frac{\mu_0 c \mathbf{m}_0}{4\pi\lambda'^2 r} \sin\theta\hat{\phi} \times \frac{\mathbf{m}_0 \mu_0}{4\pi\lambda'^2 r} \sin\theta\hat{\theta} \right\} \quad (3.3.2)$$

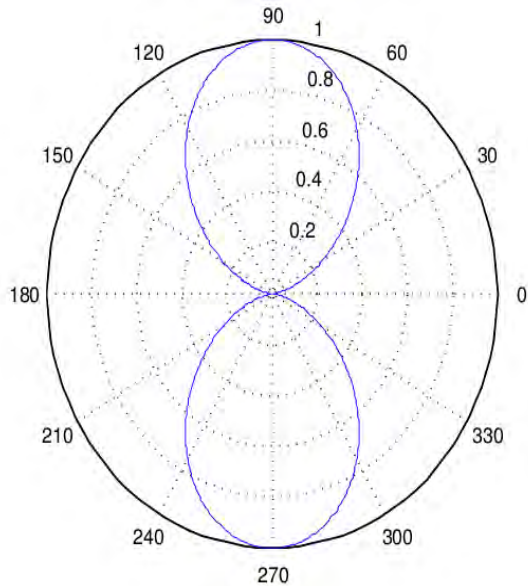
where $\hat{r} \times \hat{\phi} = -\hat{\theta}$, $\hat{\theta} \times \hat{\phi} = \hat{r}$

$$\langle s \rangle = \frac{\mu_0^2 c \mathbf{m}_0^2}{32\pi^2 \lambda'^4 r^2} \sin^2\theta\hat{r} \quad (3.3.3)$$

where $\lambda' = \frac{\lambda}{2\pi} = \frac{c}{\omega}$

$$\langle s \rangle = \frac{\mu_0^2 \omega^4 \mathbf{m}_0^2}{32c^3 \pi^2 r^2} \sin^2\theta\hat{r} \quad \text{watts/meter}^2 \quad (3.3.4)$$

Is the poynting vector that comes from dipolar electromagnetic radiation the radiation pressure with our assumption

Figure 3.2: Polar diagram of $\sin^2 \theta$

$$\langle s \rangle = \frac{\mu_0^2 \omega^4 (9 \times 10^{24})^2}{32c^3 \pi^2 r^2} \sin^2 \theta \hat{r} \quad \text{watts/meter}^2 \quad (3.3.5)$$

The average poynting vector at a distance $r \gg \lambda'$ of an oscillating magnetic dipole situated at origin. The radial distance from the dipole of the surfaces is proportional to the magnitude of the quantity in the corresponding direction. There is zero field and zero power flow along the axis. This $\frac{1}{r^2}$ dependence result from the fact that the radiation terms for E and for B both varies as $\frac{1}{r}$ since the energy flow varies as $\sin^2 \theta$, it goes to zero along the along the equator of the ring and maximum along the polar plane

3.4 Radiation Pressure Of Dipole Fields

Radiation pressure is the pressure exerted upon any surface exposed to electromagnetic radiation. If absorbed, the pressure is the power flux density divided by the speed of light. The poynting vector divided by the square of the speed of light in free space is the density of the linear momentum of the electromagnetic field. The time-averaged intensity $\langle s \rangle$ divided by the speed of light in free space is the radiation pressure exerted

by an electromagnetic wave on the surface of a target:

$$P_{rad} = \frac{\langle s \rangle}{c} \quad (3.4.1)$$

Substituting the value of poyinting vector

$$P_{rad} = \frac{\mu^2 w^4 m_0^2}{32c^4 \pi^2 r^2} \sin^2 \theta pa \quad (3.4.2)$$

We can approximate the radiation pressure according to he assumption as

$$P_{rad} = \frac{\mu^2 w^4 (9 \times 10^{24})^2}{32c^4 \pi^2 r^2} \sin^2 \theta pa \quad (3.4.3)$$

3.5 Magnetic Quadrapole Radiation

In the previous section we studied an oscillating magnetic dipole consisting loop centered on the origin and carrying an alternating current we now go on to the more elaborate type of radiation produced by a linear quadrapole whose moment is sinusoidal function of the time. We can now form an oscillating magnetic quadrapole with two such loops parallel to each other on either side of the origin and oscillating in opposite phase. The fields at the point (r, θ, φ) will differ slightly in direction, in amplitude, and in phase. We may easily neglect the difference in direction and in amplitude for $r \gg a$, but not the difference in phase to show this in detail, we shall consider the simplest case in which the distance between the loops is equal to the radius a of the loops, the two dipoles displaced from the origin by $+a/2$ and $-a/2$, and moment of the individual dipoles $-m_0 e^{i\omega t}$ and $+m_0 e^{i\omega t}$ respectively

The radiation from dipole one is closer to the field point p than in the origin by approximately $x = \frac{a}{2} \cos \theta$ similarly dipole two is further the field point by the same amount. Therefore, the phase of dipole one is relative to the origin is $+\frac{ka}{2} \cos \theta$ where $k = w/c$ on the same way the phase of dipole two relative to the origin is $-\frac{ka}{2} \cos \theta - \pi$, where the phase factor $-\pi$ enters since the two dipoles are assumed to be oscillate exactly

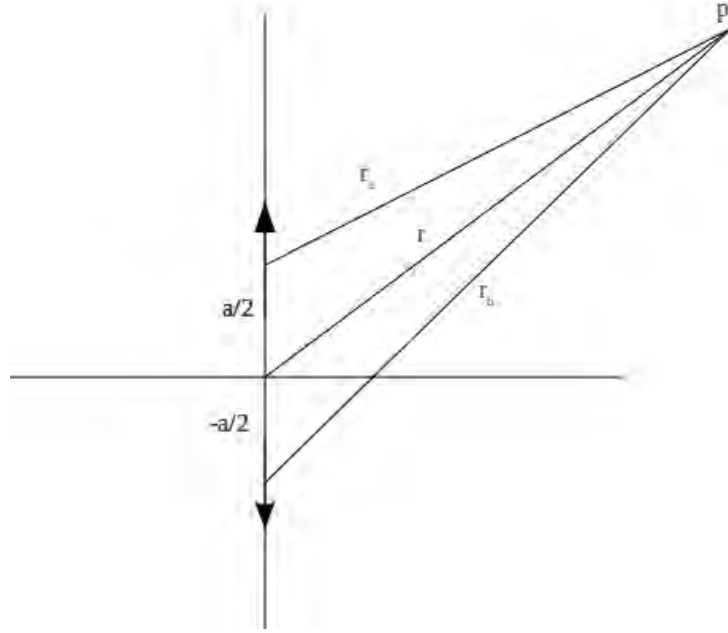


Figure 3.3: The two dipoles magnetic moment

out of phase. The ϕ component of electric field for the dipole pair is

$$\mathbf{E}_\phi = \frac{\mu_0 c \mathbf{m}_o}{4\pi r \lambda^2} e^{iw[t]} \sin \theta \left\{ e \left[i \left(\frac{ka}{2} \cos \theta \right) \right] + e \left[-i \left(\frac{ka}{2} \cos \theta + \pi \right) \right] \right\} \quad (3.5.1)$$

$$\mathbf{E}_\phi = \frac{\mu_0 c \mathbf{m}_o}{4\pi r \lambda^2} e^{iw[t]} \sin \theta \left\{ e \left[i \left(\frac{ka}{2} \cos \theta \right) \right] - e \left[-i \left(\frac{ka}{2} \cos \theta \right) \right] \right\}$$

where, we have used $e^{-i\pi} = -1$ Here is the curly brackets be come

$$\left\{ e \left[i \left(\frac{ka}{2} \cos \theta \right) \right] - e \left[-i \left(\frac{ka}{2} \cos \theta \right) \right] \right\} = 2i \sin \left(\frac{ka}{2} \cos \theta \right) \quad (3.5.2)$$

Where the Euler's formula states that, for any real number x,

$$e^{ix} = \cos x + i \sin x \quad (3.5.3)$$

$$e^{ix} - e^{-ix} = 2i \sin x \quad (3.5.4)$$

$$\mathbf{E}_\phi = \frac{\mu_0 c \mathbf{m}_o}{4\pi r \lambda^2} e^{iw[t]} \sin \theta 2i \sin \left(\frac{ka}{2} \cos \theta \right)$$

$$\begin{aligned}\mathbf{E}_\phi &= \frac{\mu_0 \mathbf{cm}_o}{2\pi r \lambda'^2} e^{iw[t]} \sin \theta i \sin\left(\frac{ka}{2} \cos \theta\right) \\ \mathbf{E}_\phi &= \frac{i\mu_0 \mathbf{cm}_o}{2\pi r \lambda'^2} e^{iw[t]} \sin \theta \sin\left(\frac{ka}{2} \cos \theta\right)\end{aligned}\quad (3.5.5)$$

If the distance between the two dipole is very small that means just considering as one point. So the value of $\frac{ka}{2} \cos \theta$ when the distance a small the value of $\sin\left(\frac{ka}{2} \cos \theta\right)$ is approximate to $\frac{ka}{2} \cos \theta$ and substitute this value in to the last expression we get

$$\mathbf{E}_\phi = \frac{i\mu_0 \mathbf{cm}_o}{2\pi r \lambda'^2} e^{iw[t]} \sin \theta \frac{ka}{2} \cos \theta \quad (3.5.6)$$

$$\mathbf{E}_\phi = \frac{i\mu_0 \mathbf{cm}_o ka}{4\pi r \lambda'^2} e^{iw[t]} \sin \theta \cos \theta \quad (3.5.7)$$

Similarly the magnetic field of the quadrapole will be calculated with the same approach to that of the electric quadrapole field.

Therefore, the sum of two dipole magnetic field

$$\mathbf{B}_\theta = -\frac{\mu_0 \mathbf{m}_0}{4\pi r \lambda'^2} e^{iw[t]} \sin \theta \left\{ e^{\left[i\frac{ka}{2} \cos \theta\right]} + e^{\left[-i\frac{ka}{2} \cos \theta + \pi\right]} \right\} \hat{\theta} \quad (3.5.8)$$

$$\mathbf{B}_\theta = -\frac{\mu_0 \mathbf{m}_0}{4\pi r \lambda'^2} e^{iw[t]} \sin \theta \left\{ e^{\left[i\frac{ka}{2} \cos \theta\right]} - e^{\left[-i\frac{ka}{2} \cos \theta + \pi\right]} \right\} \hat{\theta} \quad (3.5.9)$$

since $\exp(-i\pi) = -1$ after the applying of euler formula and considering small distance 'a' equation (3.5.12)

$$\mathbf{B}_\theta = -\frac{\mu_0 \mathbf{m}_0}{4\pi r \lambda'^2} e^{iw[t]} \sin \theta \frac{ia}{\lambda'} \cos \theta \hat{\theta} \quad (3.5.10)$$

$$\mathbf{B}_\theta = -\frac{\mu_0 \mathbf{m}_0 ia}{4\pi r \lambda'^3} e^{iw[t]} \sin \theta \cos \theta \hat{\theta} \quad (3.5.11)$$

The average poyntig vector from equation (3.3.1)

$$S_{av} = \frac{1}{2} \text{Re}(\mathbf{E} \times \mathbf{B}^*)$$

$$S_{av} = \frac{1}{2} \text{Re} \left(i \frac{\mu_0 \mathbf{cm}_0 a}{4\pi r \lambda'^3} e^{iw[t]} \sin \theta \cos \theta \times \frac{-i\mu_0 \mathbf{m}_0 a}{4\pi r \lambda'^3} e^{iw[t]} \sin \theta \cos \theta \right) \hat{r} \quad (3.5.12)$$

$$S_{av} = -\frac{1}{2} \text{Re} \left((-1) \frac{\mu_0^2 \mathbf{cm}_0^2 a^2}{16\pi^2 r^2 \lambda'^6} \sin^2 \theta \cos^2 \theta \right) \hat{r} \quad (3.5.13)$$

$$S_{av} = \left(\frac{\mu_0^2 c \mathbf{m}_0^2 a^2}{32\pi^2 r^2 \lambda^6} \sin^2 \theta \cos^2 \theta \right) \hat{r} \quad (3.5.14)$$

With our assumption the average pointing vector will approximate as

$$S_{av} = -\frac{1}{2} \text{Re} \left((-1) \frac{\mu_0^2 c (9 \times 10^{24})^2 a^2}{16\pi^2 r^2 \lambda^6} \sin^2 \theta \cos^2 \theta \right) \hat{r} \quad (3.5.15)$$

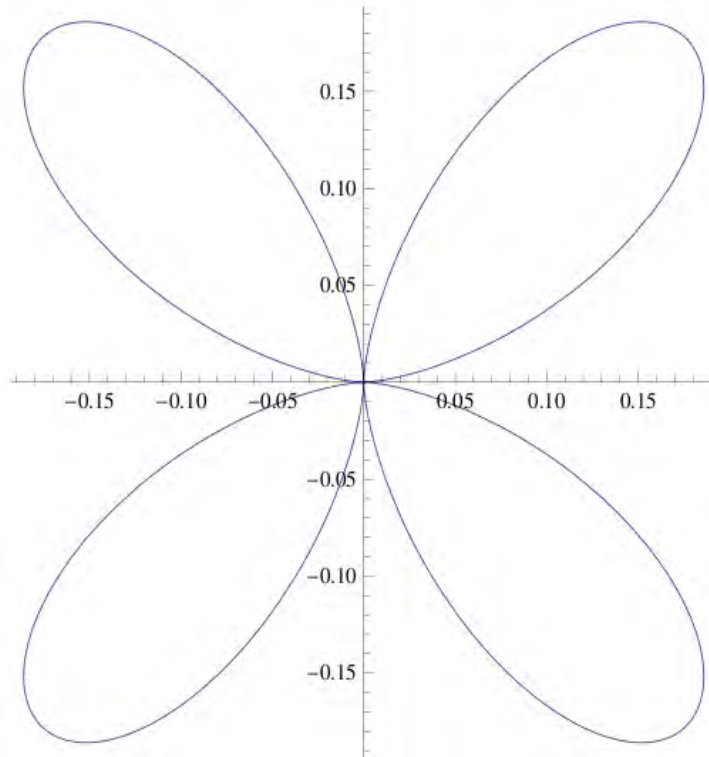


Figure 3.4: Polar diagram of $\sin^2 \theta \cos^2 \theta$

The average poyntig vector in fig (3.4) there is no field along the axis or along the equator of the quadrapole. The maximum field intensity occur along the surface of the cone at 45 degree to the axis. The quadrapole magnetic radiation are therefore oriented in the same manner as those the magnetic dipole radiation. Since we have simply superposed the fields of the two dipoles. The amplitudes of both E and B are inversely proportional to r and decrease the same rate as the dipole radiation. This makes the average poynting vector decrease again as $\frac{1}{r^2}$ therefore, the radiation pressure is

$$P_{rad} = \frac{\langle s \rangle}{c} \quad (3.5.16)$$

Substituting the value of poynting vector the radiation pressure of a quadrapole radiation is given by

$$P_{rad} = \left(\frac{\mu_0^2 c m_0^2 a^2}{32 c \pi^2 r^2 \lambda'^6} \sin^2 \theta \cos^2 \theta \right) pa \quad (3.5.17)$$

since $\lambda' = \frac{\lambda}{2\pi} = \frac{c}{w}$,

The radiation pressure;

$$P_{rad} = \left(\frac{\mu_0^2 w^6 m_0^2 a^2}{32 c^6 \pi^2 r^2} \sin^2 \theta \cos^2 \theta \right) pa \quad (3.5.18)$$

Also we can approximate the quadrapole radiation pressure

$$P_{rad} = \left(\frac{\mu_0^2 w^6 (9 \times 10^{24})^2 a^2}{32 c^6 \pi^2 r^2} \sin^2 \theta \cos^2 \theta \right) pa \quad (3.5.19)$$

Chapter 4

CONCLUSION

In the quadrupolar field line case, there is no field along the axis or along the equator of the quadrupole. The maximum field intensity occurs between zero and 90 degree. In addition to this, the quadrupole magnetic field is inversely proportional to r^4 , the dipole term in equation (3.2.5) and (3.2.9) indicates the fields E and B both varies as $\frac{1}{r}$ and this results in the average poynting vector that varies as $\frac{1}{r^2}$, this leads to a diffiuse electromagnetic radiation whose intensity is zenith-angle (θ) dependant. The intensity will go to zero only for zenit angle $\theta = 90$ degree or equipotential ring for a 3D picture of the problem. The radiation is maximum at the poles.

The quadrupole magnetic radiation are oriented in the same manner as the magnetic dipole radiation. Since we have simply superposed the fields of the two dipoles. The amplitudes of both E and B are inversely proportional to r and decrease the same rate as the dipole radiation. This makes the average poynting vector decrease again as $\frac{1}{r^2}$, The average poyntig vector for quadrupole term in equation (3.5.17) show a diffiuse electromagnetic radiation whose intensity is zenith-angle (θ) dependant. The intensity will go to zero both at the poles and at the equatorial ring. The maximum intensity occur along the surface of the cone at 45 degree. Similarly the magnetic quadrupole radiation pressure zero at poles and along the equator of the ring, and the maximum magnetic quadrupole radiation pressure occur at 45 degree.

There are two main differences between magnetic dipole and magnetic quadrupole radiation: the former field increase with the square of the frequency, whereas the latter increases as the cube of the frequency; the dipole field is zero along the poles, where as the quadrupole field is zero both at the poles at the equator.

We conclude that in general all of the result shows that the non-dipolar components of the NS magnetic field decreases quickly when the distance r is increase as compared to the dipolar component. These shows that the neutron star magnetic field has completely different structure from what we observe by approximating the neutron star magnetic field as dipolar. Specially near the surface of the NS the quadrupole component has greater contribution on the magnetic structure of the neutron star.

Reference

- [1] Bulent Kiziltan; Athanasios Kottas;Thorsett (2010). "The Neutron Star Mass Distribution".
- [2] Pawel Haensel, A Y Potekhin, D G Yakovlev (2007). Neutron Stars.
- [3] <http://ixo.gsfc.nasa.gov/images/science/neutron-stars/ns-mass-radius.gif>
- [4] V.S.Beskin (1999)."Radiopulsars"
- [5] neutron star(<http://www.daviddarling.info/encyclopedia/N/neutronstar.html>)
- [6] Baade, Walter and Zwicky, Fritz (1934). "Remarks on Super-Novae and Cosmic Rays"
- [7] L.W.Kebede 2002
- [8] Classical electro dynamics, 3rd edition,John David Jackson.
- [9] Lattimer;prakash (2010). "What atwo solar mass neutron star really means".
- [10] Hewish and Okoye; Okoye, S. E.(1965). "Evidence of an unusual source of high radio brightness temperature in of high radio brightness temperature
- [11] Shklovsky, I.S. (April 1967). "On the Nature of the Source of X-Ray Emission".
- [12] Demorest, PB; Pennucci, T; Ransom, SM; Roberts, MS; Hessels, JW (2010). "A two-solar-massneutron star measured using Shapiro delay".
- [13] Alpar, M Ali (January 1, 1998). "Pulsars, glitches and superfluids"
- [15] Posselt, B.; Neuhuser, R.; Haberl, F.(March 2009). "Searching for substellar companions of young isolated neutron stars".
- [16] electro magnetic fields and waves , 2nd edition,poul lorrain and dale corson
- [17] <http://imagine.gsfc.nassa.gov/index.html>.
- [18] <http://en.wikipedia.org/wiki/Neutron-star>
- [19] S G Gregory¹ , M Jardine² , C G Gray³ and J-F Donati⁴,The magnetic fields of forming Rep. Prog. Phys. 73 (2010) 126901 (28pp) solar-like stars
- [20] (Physics-Series) Paul-Lorrain,-Dale-R.-Corson-Electromagnetic-Fields-and-Waves-Including-Electric-Circuits -W.H.-Freeman-and-Company(1988)
- [21] "Introduction to neutron stars" (<http://www.astro.umd.edu/miller/nstar.html>) .
- [22] <http://www.iopb.res.in/phatak/em/node25.html>

Declaration

This thesis is my original work, has not been presented for a degree in any other University and that all the sources of material used for the thesis have been dully acknowledged.

Name: melkameshet girma

Signature:— — — — —

Place and time of submission: Addis Ababa University, June 2010

This thesis has been submitted for examination with my approval as University advisor.

Name: Dr. legesse wottro

Signature:— — — — —